

ChemComm

Accepted Manuscript



This is an *Accepted Manuscript*, which has been through the Royal Society of Chemistry peer review process and has been accepted for publication.

Accepted Manuscripts are published online shortly after acceptance, before technical editing, formatting and proof reading. Using this free service, authors can make their results available to the community, in citable form, before we publish the edited article. We will replace this *Accepted Manuscript* with the edited and formatted *Advance Article* as soon as it is available.

You can find more information about *Accepted Manuscripts* in the [Information for Authors](#).

Please note that technical editing may introduce minor changes to the text and/or graphics, which may alter content. The journal's standard [Terms & Conditions](#) and the [Ethical guidelines](#) still apply. In no event shall the Royal Society of Chemistry be held responsible for any errors or omissions in this *Accepted Manuscript* or any consequences arising from the use of any information it contains.

COMMUNICATION

Fe₃O₄ Nanoparticles as Robust Photothermal Agents for Driving High Barrier Reactions under Ambient Conditions*

Cite this: DOI: 10.1039/x0xx00000x

Received 00th January 2012,
Accepted 00th January 2012Robert J.G. Johnson, Kaitlin M. Haas, and Benjamin J. Lear^{a*}

DOI: 10.1039/x0xx00000x

www.rsc.org/chemcomm

Magnetite nanoparticles (MNPs) show remarkable stability during extreme photothermal heating ($\geq 770\text{K}$), displaying no change in size, crystallinity, or surfactants. The heat produced is also shown as chemically useful, driving the high-barrier thermal decomposition of polypropylene carbonate. This suggests MNPs are better photothermal agents (compared to gold nanoparticles), for photothermally driving high-barrier chemical transformations.

Heat is one of the most accessible tools for driving chemical reactions and, as such, it occupies a special place in the chemist's toolkit. However, the ultimate utility of heat – from a chemical perspective – is limited by a lack of molecular-level precision over its distribution. Recently, it was suggested that the photothermal effect (in which light is absorbed and converted to heat) of nanoparticles would allow for spatial and temporal control with nanometre and picosecond resolution.¹ The efficacy of this approach has been demonstrated for a variety of applications, such as driving reactions with large activation energies,^{2–4} breaking of the H₂ bond,⁵ chemical and materials synthesis,^{6,7} on demand phase changes in materials,⁸ evaporation of liquids,^{8–10} controlled release of drugs,^{11–19} and hyperthermal cancer treatment.^{11–13,20} While a fair amount of work on the photothermal effect of nanoparticles has focused on biological and medical applications, we are inspired by the first two examples above and our interest is in the *chemical* ramifications of this heat. We find these exciting as they demonstrate the ability to cleanly drive reactions which require

^a Prof. B. Lear
Department of Chemistry
The Pennsylvania State University
University Park, PA 16802
bul14@psu.edu

The authors would like to thank Prof. Raymond Schaak and Prof. Tom Mallouk for many helpful discussions. This work was supported through the Pennsylvania State University.

† Electronic Supplementary Information (ESI) available: Experimental details and additional characterization. See DOI: 10.1039/c000000x/

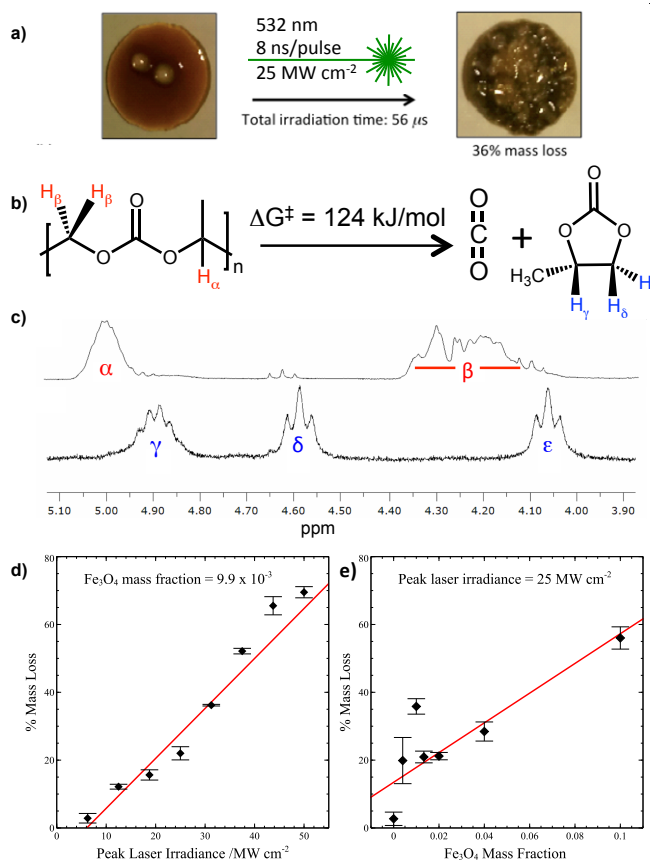


Figure 1. (a) Films of PPC with oleylamine-protected magnetite nanoparticles exposed to laser irradiation resulted in visible changes to the film. (b) These changes are a result of the degradation of PPC near the surface of the nanoparticle. (c) Production of the monomer during irradiation is verified via NMR spectra of the polypropylene carbonate (top) and condensed reaction products (bottom). Also shown are plots of the % degradation of a polymer film versus (d) peak laser irradiance and (e) concentration of magnetite nanoparticles.

temperatures well above those accessible by conventional synthetic approaches.

All of the referenced work above has employed plasmonic gold nanoparticles (AuNPs), as the surface plasmon for small (<60 nm) particles is very strongly absorptive, but very weakly luminescent.²¹ However, AuNPs also possess several critical drawbacks for photothermal applications. Gold has relatively weak metal-metal bonds, and will undergo Coulombic explosion and melting that alters the nanoparticles geometry.^{4,22-26} In addition, the Au-S and Au-N bonds commonly used to chemically modify gold nanoparticles are weak and can be broken at the high temperatures required to accomplish the exciting transformations outlined above.¹⁶

Together, the above issues preclude full control over and understanding of the mechanisms of photothermal reactions. In particular, alteration of the nanoparticle size will alter their heat capacity and absorption constant of the particles, both of which will change the ultimate temperature reached by the particles. Changes in particle shape will also alter the heat transfer properties at their surface – again altering the ability of the heat to drive changes local to the particle. Finally, the loss of ligands will change the solubility and heat transfer properties of the nanoparticle surface. Thus, poor thermal robustness of the gold nanoparticles at high temperatures prevents the molecular scale control over heat that the photothermal effect promises.

Consideration of the above problems leads to a list of desirable properties for efficient and stable photothermal agents: (i) a substantial photon absorption cross-section, (ii) strong intraparticle bonds, and (iii) strong bonds to any surfactants. In this paper, we demonstrate that magnetite (Fe₃O₄) nanoparticles (MNPs) possess all of these properties.

Figure 1 shows our approach to test the efficacy of MNPs for driving high barrier chemical reactions photothermally. Full experimental details can be found in the ESI†. In brief, MNPs were synthesized using the method of Sun et. al.²⁷ and a known mass was added to a dichloromethane solution of polypropylene carbonate (PPC). Films were cast from these solutions onto pre-weighed slides, allowed to dry, re-weighed, and then exposed to 8 ns pulses of 532 nm light from a frequency doubled Nd:YAG laser operating at a repetition of 10 Hz. The energy of individual pulses could be varied between 0 mJ and 200 mJ, in order to control the peak irradiance. Irradiation of the film resulted in a change in both the appearance and mass of the film (Figure 1a), the latter of which results from the production of volatile propylene carbonate and CO₂ (Figure 1b). – The presence of these products was verified using ¹HNMR (Figure 1c) and mass spectroscopy (see ESI†). The mass loss of the film was then used to quantify the extent of polymer degradation.

Using the film's mass loss, we then examined the efficacy of polymer degradation as a function of light irradiance (Figure 1d). For this study, films were cast with a MNPs mass fraction of 9.9×10^{-3} and then irradiated with 7,000 pulses with peak irradiances ranging from 6 to 50 MW cm⁻². Figure 1d shows a linear dependence of the percent mass loss upon the intensity of the beam, with no saturation of the MNPs absorption up to a flux of 50 MW cm⁻², though the linear fit suggests a threshold irradiance of ~ 8 MW cm⁻² must be met in order to observe degradation. This lack of saturation threshold is the same as observed for gold nanoparticles,⁴ and reflects the strongly absorbing nature of the MNP.

We also examined the efficacy of PPC degradation as a function of MNP mass loading (Figure 1e), in which films with MNPs mass fractions ranging from 9.1×10^{-2} to 4.0×10^{-3} were exposed to 7,000 pulses (25 MW cm⁻²). In addition, we exposed pure films of PPC (without MNP) to laser pulses. No matter the laser irradiance used, the observed mass loss did not exceed 3%. We find that the percent decomposition is roughly linear over the entire range of MNP concentrations. This is different from the behaviour of AuNP-doped films, which *strongly* deviate from a linear dependence at higher nanoparticle concentration resulting from a “light-limited regime.”⁴ In AuNP samples, the front of the film screens the back of the film from incident photons. The measured extinction coefficient (see ESI† for a UV-vis spectrum) for our MNPs, 1.51×10^3 (g/mL)⁻¹ cm⁻¹, is approximately 70 times less than that of 2 nm AuNPs (1.06×10^5 (g/mL)⁻¹ cm⁻¹), which explains why we do not observe a screening effect over the range of concentration of MNPs used in this experiment. However it is interesting to note that despite such a large difference in extinction coefficient, the MNPs employed here are only $\sim 30\%$ less efficient than AuNPs at driving the thermal decomposition of PPC.⁴

Considering the observed extent of decomposition of PPC, we can estimate the temperature reached by the particles is *at least* 770 K. This estimate is obtained by using the Arrhenius equation to calculate the uniform temperature of the film (see ESI for details†) required to generate our observed extent of unimolecular decomposition of PPC within the time occupied by 7,000 pulses of light (56 μs). This approach is the same as assuming that the energy absorbed by the MNPs is instantly converted to heat and distributed evenly throughout the film. As instantaneous distribution of heat is not physically reasonable, the MNP certainly attain temperatures *significantly* higher than 770 K.

The high temperatures reached by the MNPs allow us to highlight the remarkable stability offered by MNPs as photothermal agents. As shown in the ESI (Figure S2 and S3†), AuNPs are susceptible to changes under irradiation such as aggregation, fragmentation, and melting.^{4,22-26} These changes *must* result in a loss of control over the homogeneous spatial-temporal distribution, and absolute amount of heat delivered via the photothermal effect. Thus, the major perceived advantage of using the photothermal effect of nanoparticles – the fine control over local heat – is lost for AuNPs at higher irradiances. On the other hand, the MNPs used in this study display much greater stability. We have investigated the stability of MNPs in both hexane solutions and in PPC films upon irradiation (7,000 pulses, 25 MW cm⁻¹). In what follows, we focus on the results from hexane solutions, though data showing similar results from the PPC films can be found in the ESI†.

First, we highlight the *geometric* stability of MNPs. As seen in Figure 2, we observe no change in their shape (spherical), mean diameter, or size distribution of the MNP before (5.9 ± 0.8 nm) and after irradiation (5.9 ± 0.8 nm). Though the histograms associated with these populations (obtained from at least 300 particles) do show slightly different shape, our analysis shows that this is not a *statistically* significant change in either the width or centre of the distribution. This is in stark contrast to the behaviour of AuNPs exposed to similar conditions, which experience drastic increases in both the size and heterogeneity of the particles.^{4,23}

In addition to geometric stability, *crystalline* stability is also critical to consider. It is conceivable that irradiation could result in phase or

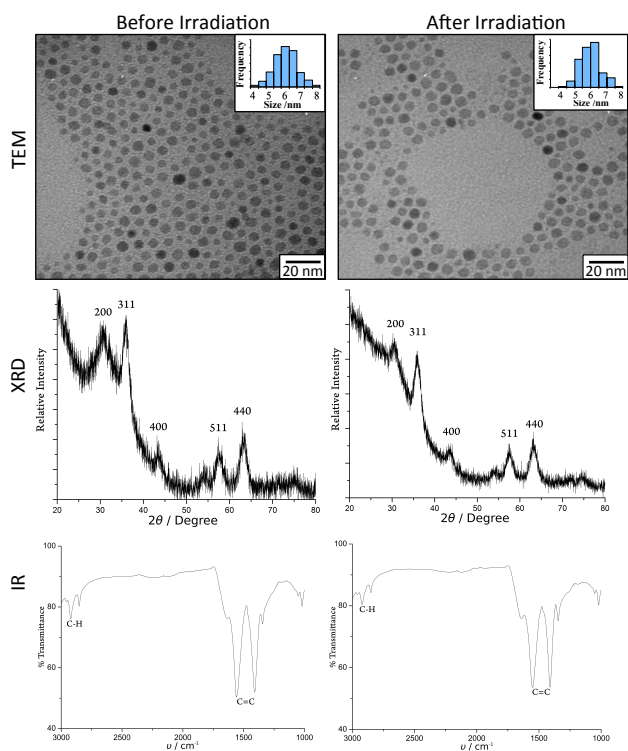


Figure 2. TEM images, XRD, and IR spectra of MNP samples before and after irradiation, showing the remarkable stability of the MNPs throughout irradiation.

composition changes of the MNPs. For example, Fe_3O_4 could become $\gamma\text{-Fe}_2\text{O}_3$.²⁸ Such transformations are undesirable, as they could alter the light absorbing and thermal properties of the MNPs. X-ray diffraction (XRD) taken before and after irradiation (Figure 2) shows the powder pattern of the MNPs remains largely unchanged, with bands at d-spacings of 2.903, 2.485, 2.076, 1.597, and 1.465 that are characteristic of Fe_3O_4 .²⁹ The only noticeable difference upon irradiation is a loss of resolution in the (220) peak, though the overall relative intensity of the (220) peak is maintained. In addition, the other peaks are not significantly broadened, which indicates that there is very little change in the crystallinity or size of the sample upon irradiation.

Beyond crystalline and size stability, the surfactants covalently attached to the MNPs were retained during irradiation – even at the extreme temperatures obtained by the MNPs. The MNPs remained soluble in hexanes throughout the irradiation – suggesting that the surfactant layer is preserved. This conclusion is supported by IR spectra taken of the dried powders used for the XRD measurements. The IR of the powders are clean and displays spectra fully consistent with the presence of oleylamine – particularly the presence of the $\nu(\text{C}=\text{C})$ stretch.

The preservation of surfactants during exposure to high photon fluency is a striking contrast to the behaviour of thiol protected AuNPs,^[11] which fall out of solution upon exposure to similar irradiances. Even without reference to the AuNPs, the preservation of the ligands at the extreme temperatures reached by the particles is remarkable. We speculate that endothermic transformations of the surroundings are functioning to protect the MNPs. In the case of the polymer, the heat sink is the endothermic depolymerisation reaction. In the case of hexanes, it is the heat of vaporization – as it is known that

plasmonic heating leads to local vaporization of solvents. For both AuNP and MNP these processes would cool the particles. We then hypothesize that the resultant temperature of the particles is sufficient to cleave the relatively weak Au-S bonds, but not the stronger bond between oleylamine and the MNPs. This hypothesis is somewhat supported by the fact that the MNP appear to be indefinitely stable in boiling hexanes, while AuNP are not. We emphasize that the above hypothesis needs testing in the future. However, the fact that it *can* be tested is a testament to the excellent surfactant stability of MNPs, which opens the door for solution-based studies into the fundamental behaviour of these nanoparticles and the possibility of preserving complex functionality of MNPs under extreme photothermal conditions.

In conclusion, we demonstrated that non-plasmonic MNPs are efficient photothermal agents for driving *chemical* reactions and offer a number of advantages over AuNPs for this application, including remarkable geometric, crystalline, and surfactant stability. This stability will prove critical for fundamental studies into the photothermal effects of nanoparticles, as well as in the design of multi-functional nanoparticles that are intended for use under these conditions. Though we are not the first to recognize the ability of MNP to function as photothermal agents,^{30–37} previous reports have focused on low temperature biological applications. We are the first to demonstrate their ability to cleanly drive specified high barrier *chemical* reactions as well as their remarkable stability under such extreme conditions. These results not only suggest that more work into the use of MNPs as photothermal agents is appropriate, but that more semiconducting and insulating nanoparticles should be examined for their efficacy and robustness as photothermal agents

Notes and references

1. A. O. Govorov, W. Zhang, T. Skeini, H. Richardson, J. Lee, and N. A. Kotov, *Nanoscale Res Lett*, 2006, **1**, 84–90.
2. C. Fasciani, C. J. B. Alejo, M. Grenier, J. C. Netto-Ferreira, and J. C. Scaiano, *Organic Letters*, 2011, **13**, 204–207.
3. J. C. Scaiano and K. Stamplecoskie, *J Phys Chem Lett*, 2013, **4**, 1177–1187.
4. K. M. Haas and B. J. Lear, *Nanoscale*, 2013, **5**, 5247–5251.
5. S. Mukherjee, F. Libisch, N. Large, O. Neumann, L. V. Brown, J. Cheng, J. B. Lassiter, E. A. Carter, P. Nordlander, and N. J. Halas, *Nano Lett*, 2013, **13**, 240–247.
6. D. A. Boyd, L. Greengard, M. Brongersma, M. Y. El-Naggar, and D. G. Goodwin, *Nano Lett*, 2006, **6**, 2592–2597.
7. J. R. Adleman, D. A. Boyd, D. G. Goodwin, and D. Psaltis, *Nano Lett*, 2009, **9**, 4417–4423.
8. C. D. Jones and L. A. Lyon, *Journal of the American Chemical Society*, 2003, **125**, 460–465.
9. Z. Fang, Y.-R. Zhen, O. Neumann, A. Polman, F. J. García De Abajo, P. Nordlander, and N. J. Halas, *Nano Lett*, 2013, **13**, 1736–1742.
10. O. Neumann, A. S. Urban, J. Day, S. Lal, P. Nordlander, and N. J. Halas, *ACS Nano*, 2013, **7**, 42–49.
11. E. C. Dreaden, M. A. Mackey, X. Huang, B. Kang, and M. A. El-Sayed, *Chem. Soc. Rev.*, 2011, **40**, 3391–3404.
12. X. Huang, I. H. El-Sayed, W. Qian, and M. A. El-Sayed, *Journal of the American Chemical Society*, 2006, **128**, 2115–2120.
13. S. Lal, S. E. Clare, and N. J. Halas, *Accounts Of Chemical Research*, 2008, **41**, 1842–1851.
14. F.-Y. Cheng, C.-H. Su, P.-C. Wu, and C.-S. Yeh, *chemical communications*, 2010, **46**, 3167–3169.
15. A. B. S. Bakhtiari, D. Hsiao, G. Jin, B. D. Gates, and N. R. Branda, *Angew Chem Int Edit*, 2009, **48**, 4166–4169.

16. L. Poon, W. Zandberg, D. Hsiao, Z. Erno, D. Sen, B. D. Gates, and N. R. Branda, *Acs Nano*, 2010, **4**, 6395–6403.
17. F. Thibaudau, *J Phys Chem Lett*, 2012, **3**, 902–907.
18. J. Huang, K. S. Jackson, and C. J. Murphy, *Nano Lett*, 2012, **12**, 2982–2987.
19. P. Matteini, F. Tatini, L. Luconi, F. Ratto, F. Rossi, G. Giambastiani, and R. Pini, *Angew Chem Int Edit*, 2013, **52**, 5956–5960.
20. L. Cheng, K. Yang, Y. Li, J. Chen, C. Wang, M. Shao, S.-T. Lee, and Z. Liu, *Angew Chem Int Edit*, 2011, **50**, 7385–7390.
21. G. F. Bohren and D. R. Huffman, *Absorption and Scattering of Light by Small Particles*, Wiley, New York, 1983.
22. P. V. Kamat, M. Flumiani, and G. V. Hartland, *J. Phys. Chem.*, 1998, **102**, 3123–3128.
23. S. Link, C. Burda, M. B. Mohamed, B. Nikoobakht, and M. A. El-Sayed, *The Journal of Physical Chemistry A*, 1999, **103**, 1165–1170.
24. S. Link, C. Burda, B. Nikoobakht, and M. El-Sayed, *Chem Phys Lett*, 1999, **315**, 12–18.
25. S. Inasawa, M. Sugiyama, and Y. Yamaguchi, *The Journal of Physical Chemistry B*, 2005, **109**, 3104–3111.
26. E. Y. Hleb and D. O. Lapotko, *Nanotechnology*, 2008, **19**, 355702.
27. S. Sun, H. Zeng, D. B. Robinson, S. Raoux, P. M. Rice, S. X. Wang, and G. Li, *Journal of the American Chemical Society*, 2004, **126**, 273–279.
28. O. N. Shebanova and P. Lazor, *J. Raman Spectrosc.*, 2003, **34**, 845–852.
29. R. Y. Hong, T. T. Pan, and H. Z. Li, *Journal of Magnetism and Magnetic Materials*, 2006, **303**, 60–68.
30. J. Kim, J. Oh, H. W. Kang, M. D. Feldman, and T. E. Milner, *Lasers Surg. Med.*, 2008, **40**, 415–421.
31. M. Chu, Y. Shao, J. Peng, X. Dai, H. Li, Q. Wu, and D. Shi, *Biomaterials*, 2013, **34**, 4078–4088.
32. L. K. Bogart, A. Taylor, Y. Cesbron, P. Murray, and R. Lévy, *Acs Nano*, 2012, **6**, 5961–5971.
33. Y. Jin, C. Jia, S.-W. Huang, M. O'Donnell, and X. Gao, *Nature Communications*, 2010, **1**, 1–8.
34. S. W. da Silva, T. F. O. Melo, M. A. G. Soler, E. C. D. Lima, M. F. da Silva, and P. C. Morais, *IEEE Trans. Magn.*, 2003, **39**, 2645–2647.
35. R. Gréget, G. L. Nealon, B. Vilen, P. Turek, C. Mény, F. Ott, A. Derory, E. Voirin, E. Rivière, A. Rogalev, F. Wilhelm, L. Joly, W. Knafo, G. Ballon, E. Terazzi, J.-P. Kappler, B. Donnio, and J.-L. Gallani, *Chem. Eur. J. of Chem. Phys.*, 2012, **13**, 3092–3097.
36. M. Johannsen, U. Gneveckow, K. Taymoorian, B. Thiesen, N. Waldöfner, R. Scholz, K. Jung, A. Jordan, P. Wust, and S. A. Loening, *Int J Hyperthermia*, 2007, **23**, 315–323.
37. K. Maier-Hauff, R. Rothe, R. Scholz, U. Gneveckow, P. Wust, B. Thiesen, A. Feussner, A. von Deimling, N. Waldöfner, R. Felix, and A. Jordan, *J Neurooncol*, 2006, **81**, 53–60.